Oxygen Sensors

DOI: 10.1002/ange.201004902

Luminescent Sensing of Oxygen Using a Quenchable Probe and Upconverting Nanoparticles**

*Daniela E. Achatz, Robert J. Meier, Lorenz H. Fischer, and Otto S. Wolfbeis**

Oxygen is ubiquitous in nature and essential for almost all living systems. It is of highest significance in areas such as physiology, biology, biotechnology, food science, and in marine, atmospheric, and space research, and in chemical process and production monitoring, to mention a few.[1] Optical sensors for oxygen have been particularly successful in the past years,[1,2] and often in combination with optical biosensors.[3] Luminescent oxygen-sensitive probes such as platinum(II) and palladium(II) porphyrins and metal–ligand complexes of ruthenium(II) and iridium(III) were found to be particularly useful for sensing oxygen because both luminescence intensities and lifetimes are dynamically (and fully reversibly)[4] quenched by oxygen and thus allow the determination of oxygen partial pressure (pO_2).[5] Such probes usually are incorporated in gas-permeable polymer matrices in the form of foils and paints, fiber optic systems,[6] micro- and nanoparticles[1b,2b,5b,7] (sometimes with magnetic cores[8]), or inside zeolites.[9]

Lanthanide-doped upconverting nanoparticles (UCNPs) are capable of emitting light in the visible range following photoexcitation with near-infrared (NIR) light, typically at a wavelength of 980 nm.[10] Among the various host materials for lanthanide ions (for example oxides, oxysulfides, phosphates, and fluorides),[11] sodium yttrium fluoride ($NaYF_4$) turned out to be among the most efficient ones.[12] UCNPs have several outstanding features that make them highly attractive: Their excitation is in the NIR spectral range and thus does not generate any interfering background luminescence (that is, in the visible), for example, by biomatter. Obviously, resonance scattering and Raman bands cannot interfere either. NIR light also penetrates biomatter much deeper than visible light but does not damage tissue, at least at the intensity levels that are applied for upconversion.[13] UCNPs are (photo)stable, and unlike quantum dots, they do not suffer from size-dependent color and blinking,[14] and from excitation by blue or even UV-light (which can cause a strong background signal and is prone to inner filter effects caused by absorbing species). Finally, their emission bands are fairly narrow, thus enabling such bands to be easily separated from others (notwithstanding the presence of side lines of weak but significant intensity). These features make bioassays based on the use of UCNPs particularly attractive, as outlined in the work by the groups of Niedbala,[15] Tanke,[16] Soukka,[17] and others.[18]

Remarkably, UCNPs have rarely been used for purposes of optical chemical sensing.[19] To date, almost all existing schemes for sensing oxygen are based on the (dynamic) quenching of the luminescence of appropriate probes by oxygen. However, the emission of UCNPs is not quenched at all by oxygen and thus cannot be used for direct sensing. On the other hand, the probes known to date cannot be photoexcited by NIR light nor do they give the effect of upconversion. In the sensing method presented herein, we are using UCNPs as a kind of nanolamps whose visible emission acts as the light source that is causing photoexcitation of an iridium(III) complex. The fluorescence of this complex, in turn, is dynamically quenched by oxygen.

We have chosen $NaYF_4$:Yb,Tm as the material for the UCNPs acting as nanolamps. They were prepared by the coprecipitation method.[20] The cubic form was converted (to a large extent) into the hexagonal form by annealing at 400 °C as described in the literature.[21] This temperature was chosen because annealing at higher temperatures, albeit yielding almost purely hexagonal phase nanocrystals, results in a highly aggregated material.[21] The material obtained by this method is well-suited for the purpose of sensing. Experimental details and a TEM image are given in the Supporting Information. The size of the particles thus obtained ranges from 80 to 120 nm. The X-ray diffraction pattern of the particles (Supporting Information, Figure S2) reveals the presence of a mixture of cubic and hexagonal-phase $NaYF_4$.

These UCNPs, on excitation with a 980 nm diode laser, give a dual emission with bands in the blue and red part of the spectrum (Figure 1 A). We perceived that this emission may serve as the excitation light source for a probe for oxygen, which by itself cannot be photoexcited with NIR laser light. The cyclometalated iridium(III) coumarin complex $[Ir(C_S)_2(acac)]$ C_S = 3-(benzothiazol-2-yl)-7-diethylamino-1-benzopyran-2-one,[2a] was chosen as the quenchable probe for oxygen because its absorbance has a maximum at 468 nm (Figure 1 B) that strongly overlaps the two shortwave emissions (at 455 and 475 nm) of the UCNPs. Its green to yellow luminescence (Figure 1 C) has a maximum at 568 nm, is strongly quenched by oxygen, and has only minimal overlap with the red emission of the UCNPs at wavelengths above 630 nm. As a result, band C can be easily separated from these using an interference filter.

[*] Dipl.-Chem. D. E. Achatz, Dipl.-Chem. R. J. Meier, Dipl.-Chem. L. H. Fischer, Prof. O. S. Wolfbeis
Institute of Analytical Chemistry, Chemo- and Biosensors
University of Regensburg, 93040 Regensburg (Germany)
E-mail: otto.wolfbeis@chemie.uni-r.de

[**] D.E.A. thanks the German Research Council (DFG, Bonn) for a stipend as part of the graduate college GRK 640 (Natural and Artificial Photoreceptors). We wish to thank S. M. Borisov (TU Graz) for kindly providing the oxygen probe $[Ir(C_S)_2(acac)]$.

Supporting information for this article is available on the WWW under http://dx.doi.org/10.1002/anie.201004902.

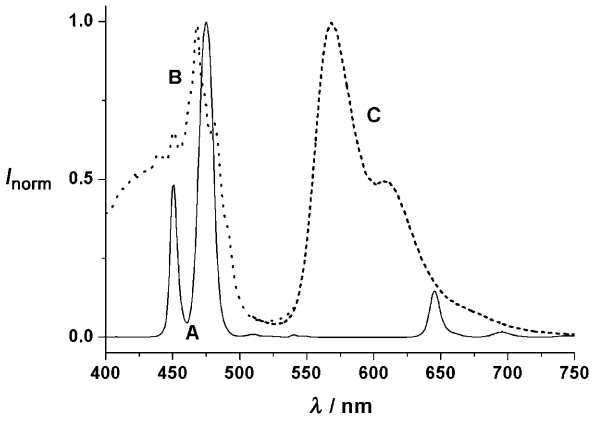

Figure 1. Normalized absorption and emission spectra showing the spectral overlap of the emission of the $NaYF_4$:Yb,Tm nanoparticles with the absorption of the oxygen probe [$Ir(C_5)_2$(acac)]. A) Emission spectrum of the nanoparticles in an ethyl cellulose matrix after photoexcitation at 980 nm with a continuous-wave 3 W diode laser; B) absorbance, and C) emission spectrum of [$Ir(C_5)_2$(acac)].

To obtain a sensor layer for continuous sensing of oxygen, the UCNPs and the oxygen probe were incorporated in a thin layer of ethyl cellulose (EC) as described in the Supporting Information. EC is easily penetrated by oxygen,[22] the permeability coefficient P being 11×10^{-13} $cm^2\,(s\,Pa)^{-1}$. The sensor film was prepared by first dissolving the iridium(III) probe, the UCNPs and EC in tetrahydrofuran, then spreading this mixture onto a glass plate, and then leaving the solvent to evaporate. The resulting yellow and slightly opaque sensor film (with a thickness of 1.8 to 2.0 μm) was placed in a flow-through cell to acquire luminescence spectra and to study quenching by molecular oxygen by passing gases with varying fractions of oxygen over it.

Figure 2 shows the emission spectra of the sensor film between 500 and 625 nm after excitation at 980 nm with a continuous wave diode laser (3 W) in an atmosphere of argon and in a gas that contains 80 % nitrogen and 20 % oxygen. The emission of the iridium complex with its maximum at 568 nm (bands C1 and C2) is quenched by oxygen. The appearance of the luminescence of the probe [$Ir(C_5)_2$(acac)] proves that the probe is photoexcited by the emission of the nanoparticles, even though the luminescence quantum yields of UCNPs are rather small,[23] typically less than 1%. The complete emission spectrum (from 400 to 750 nm) is shown in the Supporting Information (Figure S3). Compared to Figure 1, the intensities of the emission bands of the UCNPs that peak at 455 and 475 nm (bands A and B in Figure S3 in the Supporting Information) are significantly reduced in intensity, because they are absorbed (screened off) by the iridium(III) complex. The intensities of the red bands (D and E in Figure S3 in the Supporting Information) of the UCNPs and their ratio remain unaffected, but their relative contributions to the overall emission are of course much larger now.

We interpret this effect to be a result of the UCNPs acting as nanolamps inside the sensor film, with their blue emission being absorbed (and converted into green–yellow luminescence) by the iridium complex. Fluorescence resonance energy transfer[24] (as invoked in cases where upconverting particles were used as labels in bioassays)[13b,17,25] is unlikely to occur to a substantial extent given the average distance between the two emitters, which is far above the Förster distance of typically 7–10 nm. This fact has also been pointed out by Morgan et al.[26]

A more careful look at bands C1 and C2 in Figure 2 reveals that there is a small contribution (a shoulder on the left side of the band) that originates from the UCNPs, probably a result of the presence of traces of erbium(III) ions.

The respective Stern–Volmer plots[5a] (Figure 3; average of five independent measurements for each oxygen concentration) reveal three interesting findings: 1) The Stern–Volmer plot resulting from direct excitation of the iridium probe is highly linear, whereas that of the indirectly excited probe is strongly curved; 2) the slopes of the Stern–Volmer

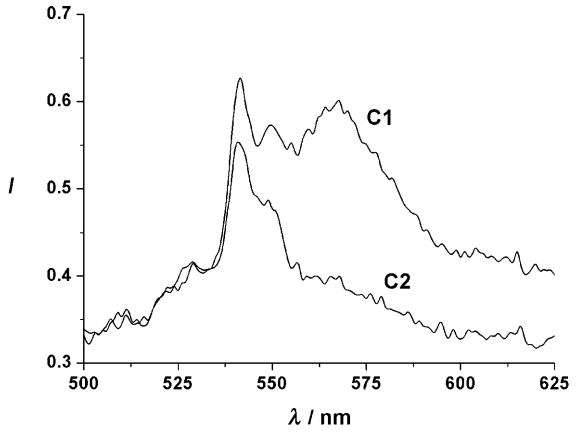

Figure 2. Visible emission spectra of an ethyl cellulose sensor film containing the $NaYF_4$:Yb,Tm upconverting nanoparticles (UCNPs) and the oxygen probe [$Ir(C_5)_2$(acac)] following photoexcitation at 980 nm. The decrease in size of the peak at 568 nm (C1) in argon, (C2) after exposure to argon containing 20% oxygen) clearly indicates the quenching of [$Ir(C_5)_2$(acac)] by oxygen. $T = 24$ °C; atmospheric pressure.

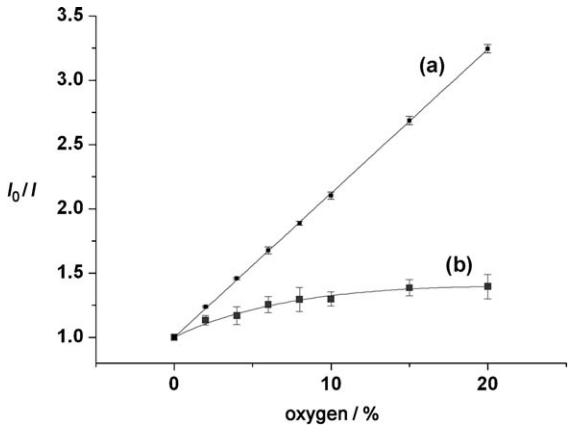

Figure 3. Stern–Volmer plots of the quenching by oxygen of the emission of an ethyl cellulose sensor film containing the oxygen probe [$Ir(C_5)_2$(acac)] and the $NaYF_4$:Yb,Tm UCNPs. Plot (a) was obtained after direct excitation of the iridium probe at 475 nm by using a xenon lamp, and plot (b) was obtained after diode laser excitation of the UCNPs at 980 nm and monitoring the green emission of the iridium probe.

plots differ strongly depending on whether the sensor film is excited conventionally at 475 nm (using a xenon lamp; see plot A), or whether excitation is performed at 980 nm by the nanoparticles (plot B); and 3) the precision (expressed as the standard deviation; see Figure 4) is much higher for conventional excitation. This shall be discussed and interpreted below and in the Supporting Information.

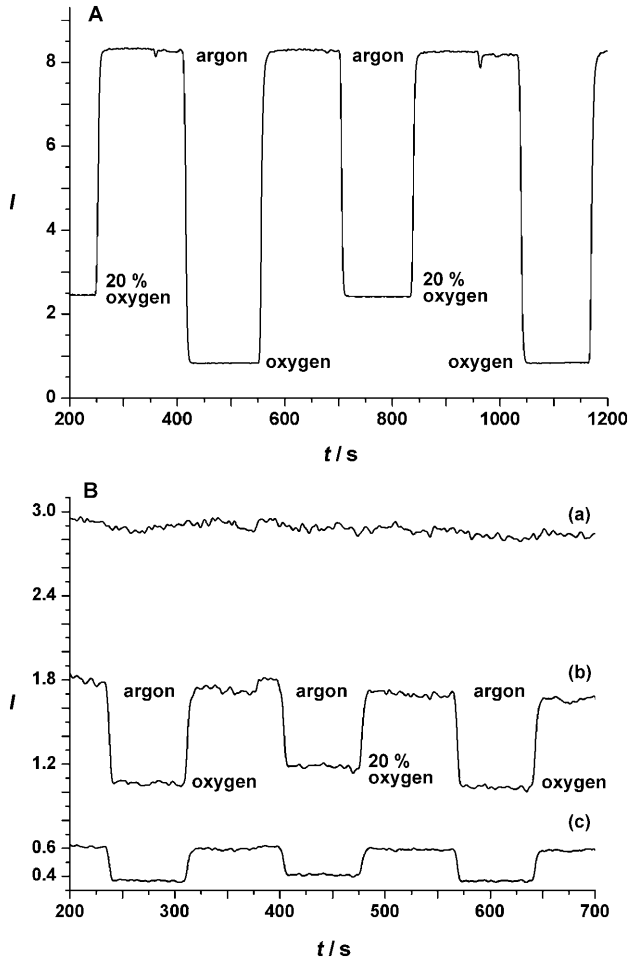

Figure 4. Time traces obtained with the oxygen sensor film and showing response times, reversibility, and relative signal changes. A) Signal obtained by direct photoexcitation of the Ir^{III} oxygen probe at 475 nm using a xenon lamp and cycling between argon, nitrogen containing 20% oxygen, and oxygen. B) Signal obtained under photoexcitation of the UCNPs at 980 nm and recording the green emission of the iridium probe at 568 nm. Time traces were obtained by cycling between argon, nitrogen with 20% oxygen, and pure oxygen. Emissions were collected at 696 nm (trace (a)) and at 568 nm (trace (b)). Plot (c) gives the (much less noisy) ratio of the two signals (I_{568}/I_{696}).

Both the difference in the slope and in the shape of the plots can be interpreted in terms of different microenvironments of the iridium-based probes for oxygen. Illumination at 475 nm will photoexcite all of the probe molecules dissolved in ethyl cellulose. The overwhelming majority of them are freely accessible to oxygen. Dynamic quenching therefore will be highly efficient, and the respective Stern–Volmer plot (plot A in Figure 3) is linear ($\sigma^2 = 1$). The quenching constant (K_{sv}) was calculated to be $0.112\,\%^{-1}$. If, however, the sensor film is illuminated with the 980 nm diode laser, photoexcitation will occur via the luminescence of the UCNPs, which act as nanolamps inside the sensor film. As a result, probe molecules located close to the UCNP and to a lesser extent in the bulk of the film will be photoexcited. Those located close to the nanoparticles will not be freely accessible to oxygen, but rather be shielded on one side by the nanoparticles from being quenched. This will result in a distinctly reduced quenching efficiency of these molecules. This interpretation of the quenching mechanisms involved is further corroborated by the highly linear response of a sensor film containing the iridium probe only but no UCNPs.[2a] Measurements were also performed with sensor films containing different relative concentrations of UCNPs and iridium complex; the results of these experiments are given in the Supporting Information.

Figure 4 shows time traces of the signal at 568 nm with changing levels of oxygen after excitation at 475 nm (plot A) and 980 nm (plot B). In case of photoexcitation at 980 nm, the emission of the UCNPs at 696 nm also was collected (with a time delay of less than 1 s, which was caused by the instrument). The response of the sensor layer is fully reversible, and its response time is between 10 to 12 s for both excitation wavelengths. Figure 4 also reveals that the time trace obtained with conventional excitation (plot A) is more stable than the rather noisy trace obtained at 980 nm excitation (plot B, trace (b)).

The larger noise in Figure 4Bb is due to the overall weaker emission of the oxygen probe obtained by excitation at 980 nm, and thus a smaller signal-to-noise ratio (as discussed in the Supporting Information), but it is probably also due to fluctuations of the intensity of the diode laser. Such fluctuations can be eliminated, in principle, by referencing the (green) signal of the iridium probe at 568 nm to the red peak of the UCNPs at 696 nm (Figure S3 in the Supporting Information, band E). This band is neither involved in the photoexcitation nor does it overlap the emission of the iridium complex (Figure 1), and is thus an excellent reference signal that undergoes the same fluctuations as the diode laser. A fluorometer was used to determine the ratio I_{568}/I_{696} within 1 s, and indeed a much less noisy signal (see trace (c) in Figure 4B) is obtained by forming the ratio of the signal traces (a) and (b). Obviously, however, fluctuations occurring in a time regime of less than 1 s and effects of delayed emission of the nanoparticles cannot be eliminated by this method. We also suspect that the nanolamps cause local heating,[27] and this may lead to temperature-dependent differences in the intensity of the effects of temperature on the relative ratio of the two emission bands of the UCNPs and the quantum yield of the iridium probe. In fact, we presume that the slight signal drift in Figure 4B, trace (a) is partially due to local warming of the sensor film in close proximity to the UCNPs. Moreover, the temperature dependence of the particular transitions in the UCNPs is known to be non-uniform.[28]

In conclusion, the first sensor for oxygen that can be excited with NIR light has been presented. It makes use of UCNPs that are photoexcited with a 980 nm laser and the visible luminescence of which is used to photoexcite a quenchable probe for oxygen, thereby overcoming the lack

of NIR-excitable probes for oxygen. The approach complements our recently reported sensors for pH values and for ammonia,[19] which however are based on a quite different sensing method. The components and materials used are readily available, and the merits of working at such long excitation wavelength have been presented, the main benefit being the complete absence of luminescence background that can be strong in samples such as serum.[29] A new type of ratiometric readout also is demonstrated. We believe that this method can be extended to numerous other fluorescent sensing probes.

Received: August 6, 2010
Published online: October 28, 2010

Keywords: luminescence · nanoparticles · oxygen · sensor · upconversion

[1] a) A. Mills, *Chem. Soc. Rev.* **2005**, *34*, 1003 – 1011; b) X. Ge, M. Hanson, H. Shen, Y. Kostov, K. A. Brorson, D. D. Frey, A. R. Moreira, G. Rao, *J. Biotechnol.* **2006**, *122*, 293 – 306; c) N Pérez-Ortíz, F. Navarro-Villoslada, G. Orellana, F. Moreno-Jiménez, *Sens. Actuators B* **2007**, *126*, 394 – 399; d) C. Wu, B. Bull, K. Christensen, J. McNeill, *Angew. Chem.* **2009**, *121*, 2779 – 2783; *Angew. Chem. Int. Ed.* **2009**, *48*, 2741 – 2745.

[2] a) S. M. Borisov, I. Klimant, *Anal. Chem.* **2007**, *79*, 7501 – 7509; b) X. Wang, X. Chen, Z. Xie, X. Wang *Angew. Chem.* **2008**, *120, 7560–7563; Angew. Chem. Int. Ed.* **2008**, 47, 7450 – 7453; *Angew. Chem. Int. Ed.* **2008**, *47*, 7450 – 7453; *Angew. Chem.* **2008**, *120*, 7560 – 7563; c) C. McDonagh, C. S. Burke, B. D. MacCraith, *Chem. Rev.* **2008**, *108*, 400 – 422; d) G. Zhang, G. M. Palmer, M. W. Dewhirst, C. L. Fraser, *Nat. Mater.* **2009**, *8*, 747 – 751.

[3] S. M. Borisov, O. S. Wolfbeis, *Chem. Rev.* **2008**, *108*, 423 – 461.

[4] We refer to sensors here only if the response is fully reversible. In our view, so-called "molecular sensors" should be referred to as indicators, or even better as molecular probes.

[5] a) J. N. Demas, B. A. DeGraff, P. B. Coleman, *Anal. Chem.* **1999**, *71*, 793A – 800A; b) S. M. Borisov, G. Nuss, I. Klimant, *Anal. Chem.* **2008**, *80*, 9435 – 9442; c) S. M. Borisov, D. B. Papkovsky, G. V. Ponomarev, A. S. DeToma, R. Saf, I. Klimant, *J. Photochem. Photobiol. A* **2009**, *206*, 87 – 92.

[6] Review: O. S. Wolfbeis, *Anal. Chem.* **2008**, *80*, 4269 – 4283.

[7] F. Navarro-Villoslada, G. Orellana, M. C. Moreno-Bondi, T. Vick, M. Driver, G. Hildebrand, K. Liefeith, *Anal. Chem.* **2001**, *73*, 5150 – 5156.

[8] P. Chojnacki, G. Mistlberger, I. Klimant, *Angew. Chem.* **2007**, *119*, 9006 – 9009; *Angew. Chem. Int. Ed.* **2007**, *46*, 8850 – 8853.

[9] B. Meier, T. Werner, I. Klimant, O. S. Wolfbeis, *Sens. Actuators B* **1995**, *29*, 240 – 245.

[10] a) F. Auzel, *Chem. Rev.* **2004**, *104*, 139 – 173; b) E. Beurer, J. Grimm, P. Gerner, Hans U. Güdel, *J. Am. Chem. Soc.* **2006**, *128*, 3110 – 3111.

[11] a) S. Heer, O. Lehmann, M. Haase, H.-U. Güdel, *Angew. Chem.* **2003**, *115*, 3288 – 3291; *Angew. Chem. Int. Ed.* **2003**, *42*, 3179 – 3182; *Angew. Chem.* **2003**, *115*, 3288 – 3291; b) Q. Lü, F. Guo, L. Sun, A. Li, L. Zhao, *J. Appl. Phys.* **2008**, *103*, 123533; c) Y. Qu, X. Kong, Y. Sun, Q. Zeng, H. Zhang, *J. Alloys Compd.* **2009**, *485*, 493 – 496; d) A. M. Pires, O. A. Serra, M. R. Davolos, *J. Alloys Compd.* **2004**, *374*, 181 – 184.

[12] K. W. Krämer, D. Biner, G. Frei, H. U. Güdel, M. P. Hehlen, S. R. Lüthi, *Chem. Mater.* **2004**, *16*, 1244 – 1251.

[13] a) F. Wang, X. Liu, *Chem. Soc. Rev.* **2009**, *38*, 976 – 989; b) C. G. Morgan, S. Dad, A. C. Mitchell, *J. Alloys Compd.* **2008**, *451*, 526 – 529; c) Z. Li, Y. Zhang, S. Jiang, *Adv. Mater.* **2008**, *20*, 4765 – 4769.

[14] S. Wu, G. Han, D. J. Milliron, S. Aloni, V. Altoe, D. V. Talapin, B. E. Cohen, P. J. Schuck, *Proc. Natl. Acad. Sci. USA* **2009**, *106*, 10917 – 10921.

[15] P. L. A. M. Corstjens, S. Li, M. Zuiderwijk, K. Kardos, W. R. Abrams, R. S. Niedbala, H. J. Tanke, *IEE Proc. Nanobiotechnol.* **2005**, *152*, 64 – 72.

[16] P. L. A. M. Corstjens, L. van Lieshout, M. Zuiderwijk, D. Kornelis, H. J. Tanke, A. M. Deelder, G. J. van Dam, *J. Clin. Microbiol.* **2008**, *46*, 171 – 176.

[17] a) K. Kuningas, T. Ukonaho, H. Päkkilä, T. Rantanen, J. Rosenberg, T. Lövgren, T. Soukka, *Anal. Chem.* **2006**, *78*, 4690 – 4696; b) T. Rantanen, M. L. Järvenpää, J. Vuojola, K. Kuningas, T. Soukka, *Angew. Chem.* **2008**, *120*, 3871 – 3873; *Angew. Chem. Int. Ed.* **2008**, *47*, 3811 – 3813; *Angew. Chem.* **2008**, *120*, 3871 – 3873.

[18] a) A. L. Ouellette, J. J. Li, D. E. Cooper, A. J. Ricco, G. T. A. Kovacs, *Anal. Chem.* **2009**, *81*, 3216 – 3221; b) F. Vetrone, J. A. Capobianco, *Int. J. Nanotechnol.* **2008**, *5*, 1306 – 1339.

[19] a) L. Sun, H. Peng, M. I. J. Stich, D. E. Achatz, O. S. Wolfbeis, *Chem. Commun.* **2009**, 5000 – 5002; b) H. S. Mader, O. S. Wolfbeis, *Anal. Chem.* **2010**, *82*, 5002 – 5004.

[20] G. Yi, H. Lu, S. Zhao, Y. Ge, W. Yang, D. Chen, L.-H. Guo, *Nano Lett.* **2004**, *4*, 2191 – 2196.

[21] Y. Wei, F. Lu, X. Zhang, D. Chen, *J. Alloys Compd.* **2007**, *427*, 333 – 340.

[22] J. Brandrup, E. H. Immergut, E. A. Grulke, *Polymer Handbook*, 4th ed., Wiley, NY, **1999**.

[23] J.-C. Boyer, F. C. J. M. van Veggel, *Nanoscale* **2010**, *2*, 1417 – 1419

[24] J. N. Miller, *Analyst* **2005**, *130*, 265 – 270.

[25] a) T. Soukka, T. Rantanen, K. Kuningas, *Ann. N. Y. Acad. Sci.* **2008**, *1130*, 188 – 200; b) L. Wang, R. Yan, Z. Huo, L. Wang, J. Zeng, J. Bao, X. Wang, Q. Peng, Y. Li, *Angew. Chem.* **2005**, *117*, 6208 – 6211; *Angew. Chem. Int. Ed.* **2005**, *44*, 6054 – 6057.

[26] The authors of Ref. [13b] state that "assay formats other than FRET are possible and in particular near-field coupling of upconverted emission to conventionally labeled microspheres or energy transfer from 'whispering gallery' modes at the surface of upconverting microspheres are … possible alternatives."

[27] V. K. Tikhomirov, K. Driesen, V. D. Rodriguez, P. Gredin, M. Mortier, V. V. Moshchalkov, *Opt. Express* **2009**, *17*, 11794 – 11798.

[28] S. A. Wade, S. F. Collins, G. W. Baxter, *J. Appl. Phys.* **2003**, *94*, 4743 – 4756.

[29] O. S. Wolfbeis, M. Leiner, *Anal. Chim. Acta* **1985**, *167*, 203 – 215.

